

## THE RELATION BETWEEN THE TRANSIT DEPTHS OF KIC 12557548B & THE STELLAR ROTATION PERIOD

BRYCE CROLL<sup>1,2</sup>, SAUL RAPPAPORT<sup>2</sup>, ALAN M. LEVINE<sup>2</sup>

*Draft version December 4, 2021*

### ABSTRACT

Kawahara and collaborators analyzed the transits of the candidate disintegrating Mercury-mass planet KIC 12557548b and suggested that the transit depths were correlated with the phase of the stellar rotation. We analyze the transit depths of KIC 12557548b and confirm that there is indeed a robust, statistically significant signal in the transit depths at the rotation period of the spotted host star. This signal is more prominent in the first-half of the *Kepler* data, and is not due to leakage of the rotating spot signal into our measurement of the transit depths, or due to unocculted starspots. We investigate the suggestion that this signal could be due to an active region on the star, emitting enhanced ultraviolet or X-ray radiation leading to an increased mass loss rate of the planet; we confirm that such a scenario could cause both modulation of the transit depths of KIC 12557548b, and small enough transit-timing variations that they might not be detected in the *Kepler* data. Our preferred explanation for the fact that the transit depths of KIC 12557548b are modulated with the stellar rotation phase is that the candidate transiting planet is occulting starspots on this highly spotted star; such a scenario could cause transit depth variations as large as have been observed, and cause transit-timing variations small enough that they are arguably consistent with the *Kepler* data.

*Subject headings:* planetary systems . stars: individual: KIC 12557548

### 1. INTRODUCTION

The unprecedented precision of the *Kepler* space telescope's (Borucki et al. 2009; Koch et al. 2011) photometry has resulted in the discovery of a wealth of intriguing exoplanet systems; one such system is the candidate disintegrating Mercury-mass exoplanet KIC 12557548b (Rappaport et al. 2012). The *Kepler* photometry of the K-dwarf host star KIC 12557548 (hereafter referred to as KIC 1255, while the exoplanet will be denoted KIC 1255b) displays dips that repeat every  $\sim 15.7$  hours that vary in depth from being undetectably shallow to as large as 1.3% of the host star's flux. Intriguingly, KIC 1255b's transit profile displays a sharp ingress, followed by a gradual egress; for these reasons, Rappaport et al. (2012) suggested that KIC 1255b may feature a long cometary tail streaming behind the candidate planet. In this scenario, KIC 1255b's transits are believed to be caused by light being scattered out of the line-of-sight from small particles<sup>3</sup> trailing behind the planet. The variable transit depths were suggested to be due to different amounts of material being ejected from the planet for each orbit.

Such an interesting system has quickly resulted in a number of follow-up observations and re-analyses of the original *Kepler* data. These include reanalyses of the *Kepler*-data largely supporting the disintegrating planet scenario (Brogi et al. 2012; Budaj 2013; van Werkhoven et al. 2014), theoretical efforts exploring the disintegration of the planet

(Perez-Becker & Chiang 2013), and comparisons of the depth of the transits of KIC 1255b obtained in the optical with *Kepler*, to those obtained in the near-infrared with the Canada-France-Hawaii Telescope (Croll et al. 2014). Perhaps the biggest unresolved issue presented by all the follow-up efforts, has been the suggestion that KIC 1255b's transit depth variations are correlated with the phase of the stellar rotation period (Kawahara et al. 2013).

In the original Rappaport et al. (2012) paper the authors were not able to identify a pattern to explain the dramatic variability of KIC 1255b's transit depths. Kawahara et al. (2013) analyzed KIC 1255b's transit depths and presented evidence that the observed transit depths were modulated at the stellar rotation period ( $P_{rot} \sim 22.9$  d); the authors found that the transits were on average 30% deeper during one phase of the stellar rotation than another. Kawahara et al. (2013) went on to suggest that the presumed variable mass loss rate of the planet may therefore be a byproduct of the stellar activity, and related to an active longitude or starspot group on the star. In the Kawahara et al. (2013) scenario, when the planet passes over this active region it may be subjected to increased ultraviolet and X-ray radiation, or some sort of star-planet interaction arising from magnetic reconnection, leading to an increased mass-loss rate. However, one problem that quickly arises with the proposed explanation is that even though an active longitude on the star would only be visible to an observer on the Earth once per stellar rotation period, the planet would pass over this active longitude each and every orbit. The travel time for dust grains to pass from the planet to the end of the cometary tail is expected to be of the order of an orbital period, while an estimate for the sublimation lifetime of the grains is several hours (Rappaport et al. 2012); therefore even if there were an

<sup>1</sup> 5525 Olund Road, Abbotsford, B.C. Canada

<sup>2</sup> Kavli Institute for Astrophysics and Space Research, Massachusetts Institute of Technology, Cambridge, MA 02139, USA; croll@space.mit.edu

<sup>3</sup> Originally thought to be sub-micron-sized particles, although Croll et al. (2014) suggest the largest particles in the cometary tail should be  $\sim 0.5 \mu\text{m}$  or larger.

active longitude on the star causing increased disintegration of the planet – either from blasting the planet with intense ultraviolet or X-ray radiation, or subjecting it to some sort of magnetic star-planet interaction – the effects would be spread over a significant duration of the extremely short  $\sim 15.7$  hour orbital period of the planet.

More benign explanations for the observed relation include the effects of occulted and unocculted starspots, or leakage from the significant rotational starspot modulation of KIC 1255 causing mis-estimates of KIC 1255b’s transit depths. KIC 1255 displays obvious rotational modulation with peak to peak variations between  $\sim 1\%$  and  $\sim 5\%$  of the observed stellar flux with a rotation period of  $\sim 22.9$  d. Unocculted and occulted spots are known to bias the measurements of transit depths (e.g. Czela et al. 2009; Carter et al. 2011); furthermore, if the significant rotational modulation leaks into measurements of the planet’s transit depths, the reported signal could simply be an artefact. Kawahara et al. (2013) considered the possibility that unocculted spots could introduce a correlation between KIC 1255b’s transit depths and the rotation period, but suggested that the 30% transit depth signal was far greater than would be expected for unocculted spots.

In this paper we attempt to verify whether the claimed KIC 1255 Transit Depth - Rotation Modulation Signal (hereafter referred to as the TDRM signal) is genuine, and if it is due to something more astrophysically interesting than simply occulted and unocculted spots. In Section 2 we demonstrate that the TDRM signal is not due to an artefact, and is statistically significant; however, we show that other spotted stars also display a similar signal due to occulted spots. We also present a transit-timing analysis of the transits of KIC 1255b. In Section 3 we examine three scenarios for the TDRM signal. We rule out unocculted spots, and demonstrate that the scenario suggested by Kawahara et al. (2013) – of an active region with enhanced ultraviolet radiation leading to an increased mass loss rate – could naturally cause the transit depth variations that are observed. However, we argue that occulted spots are arguably the simplest explanation presented to date for the TDRM signal.

## 2. ANALYSIS OF THE TRANSIT DEPTH ROTATIONAL MODULATION SIGNAL

### 2.1. Basic analysis

We first largely repeat the analysis presented in Kawahara et al. (2013) using our own techniques. We start by analyzing the *Kepler* long cadence ( $\sim 29.4$  minute sampling) photometry of KIC 1255 (quarters 1-17)<sup>4</sup>. We utilize the pre-search data conditioning simple aperture photometry (PDCSAP; Smith et al. 2012; Stumpe et al. 2012) of this star. We normalize the light curve for each *Kepler* quarter to the median flux observed in that quarter. The success of our analysis depends on ensuring that the transit depths of KIC 1255b are accurately measured despite KIC 1255’s obvious rotational flux modulation. In order to ensure that this is the case, we remove the rotational modulation by subtracting out a cubic spline fit. To ensure that the asymmetrical transit of KIC 1255b does not affect our removal of the ro-

<sup>4</sup> Our analysis features two quarters of data that were not available at the time of the Kawahara et al. (2013) analysis.

TABLE 1  
ANALYSIS PARAMETERS

Star	$\phi_{mincut}$	$\phi_{maxcut}$	sigma-cut	$P_{orbit}$ (d)	$P_{rot}$ (d)
KIC 1255	0.40	0.60	$10\sigma$	$\sim 0.65$	$\sim 22.9$
Kepler-17	0.45	0.55	n/a	$\sim 1.49$	$\sim 12.3$
HAT-P-11	0.48	0.52	n/a	$\sim 4.89$	$\sim 30.0$
Kepler-78	0.40	0.60	n/a	$\sim 0.36$	$\sim 12.8$

tational modulation, we cut out all data in the transit before calculating our cubic spline. That is, we phase the data to the orbital period of the candidate planet (where phase,  $\phi=0.5$  denotes the midpoint of the transit), and cut out all data between phases of  $\phi_{mincut} = 0.4$  to  $\phi_{maxcut}=0.7$ . We then bin the data every  $\sim 10$  hr, and use these data to calculate our cubic spline, and remove the obvious rotational modulation. We apply a  $10\sigma$  cut to the spline-corrected data to remove obvious outliers. Relevant analysis parameters are summarized in Table 1. The photometric data of KIC 1255 before and after the removal of the rotational modulation are displayed in the top panels of Figure 1.

Kawahara et al. (2013) measured the transit depths of KIC 1255b by averaging the three long cadence *Kepler* points nearest to the mid-point of the transit, and we do likewise. This method has the obvious drawback of imprinting the frequency of the long cadence photometry into the transit signal, but as we are interested in a signal with a much longer period than the  $\sim 29.4$  minute cadence of long cadence photometry, this effect does not seriously impact our science goals. We have experimented with formally fitting the transit depths of KIC 1255b, as we do in Croll et al. (2014), and we’ve confirmed that the results are similar to the method we use here.

We then take a Lomb Scargle periodogram (Lomb 1976; Scargle 1982) of the KIC 1255b transit depths (bottom right panel of Figure 1). Similarly to Kawahara et al. (2013) we notice a modest peak in the periodogram near the rotation period of the star<sup>5</sup>. The peak at  $\sim 0.65$  d is simply due to the orbital period of the planet. There are more prominent peaks in the periodogram at longer periods than the rotation period; these periods were also mentioned in Kawahara et al. (2013). These longer period peaks are largely due to the quiescent periods at the start and the end of the data-set when the KIC 1255b transit depths are virtually undetectable (these quiescent periods were noted in van Werkhoven et al. 2014). If we repeat the analysis excluding these points – by excluding data before BJD = 2455078.0 and data after BJD = 2456204.3 – the results are shown in Figure 2. There does appear to be a prominent peak in the periodogram near the rotation period of the star.

#### 2.1.1. Further investigation of the suggested TDRM signal

We also phase the transit depths, excluding those data before and after the quiescent periods (Figure 2), to the

<sup>5</sup> We determine the rotation period of the star by identifying the maximum peak in the Lomb Scargle periodogram of the *Kepler* long cadence data, once the transit data has been removed from  $\phi_{mincut}$  to  $\phi_{maxcut}$ , as given in Table 1.

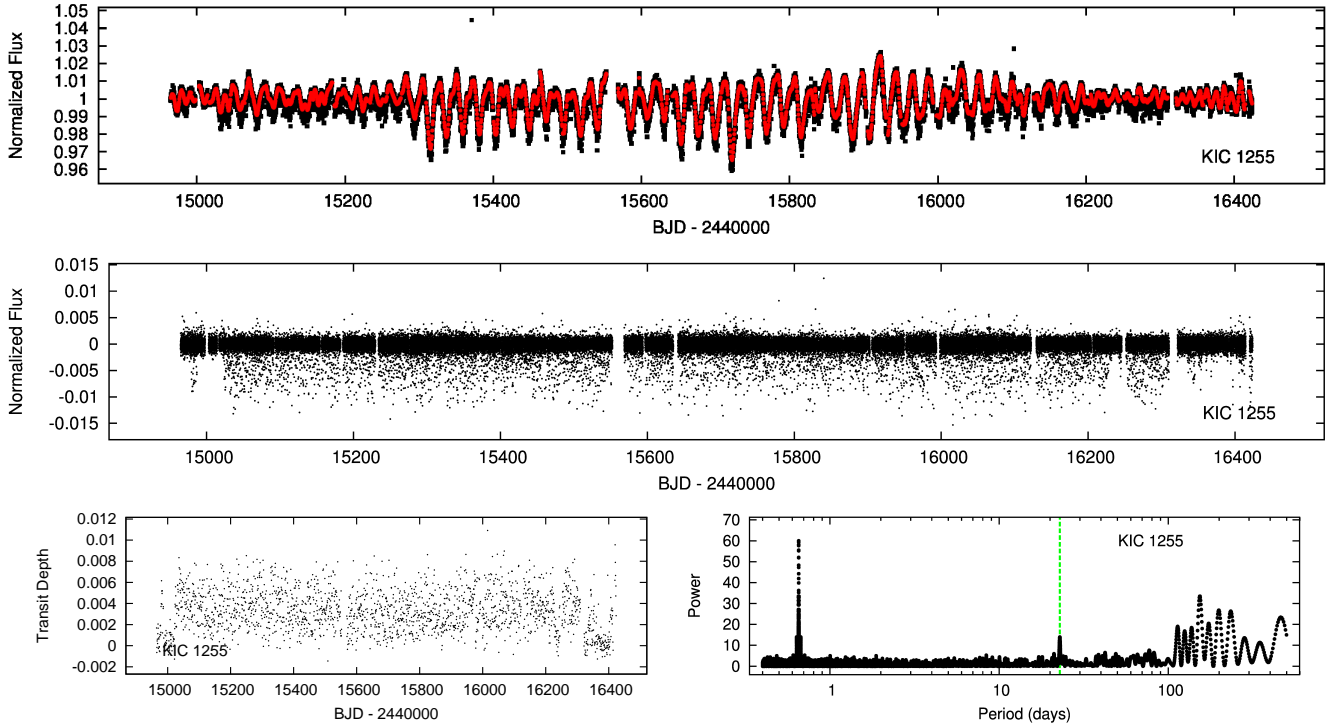


FIG. 1.— Top panel: The *Kepler* long cadence photometry of KIC 1255 (black points); the red points display the values used in the cubic spline fit to subtract out KIC 1255’s obvious rotational modulation. Middle panel: The *Kepler* long cadence photometry after the subtraction of the spline fit to remove the obvious rotational modulation. The transits every  $\sim 15.7$  hours of KIC 1255b are obvious as the sea of points just below the mean of the light curve. Bottom left panel: The transit depths of the *Kepler* long cadence photometry of KIC 1255b. Bottom right panel: The Lomb Scargle periodogram of the transits of KIC 1255b. The vertical dotted green line displays the  $\sim 22.9$  d rotation period of KIC 1255.

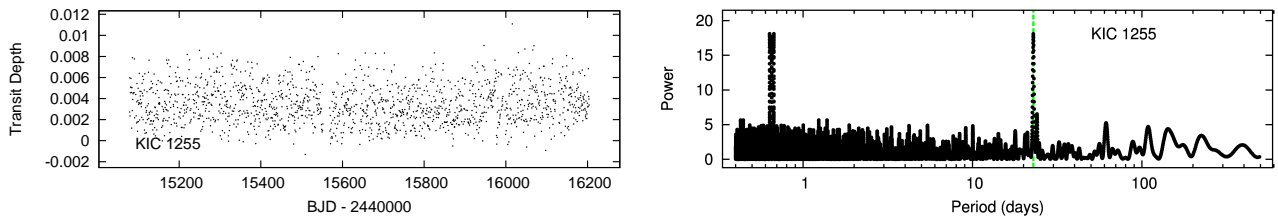


FIG. 2.— Left panel: The transit depths of the *Kepler* long cadence photometry of KIC 1255b, excluding the quiescent periods, by cutting all data before BJD = 2455078.0 and after BJD = 2456204.3. Right panel: The associated Lomb Scargle periodogram of the transits of KIC 1255b. The vertical dotted green line displays the  $\sim 22.9$  d rotation period of KIC 1255.

rotation period of the star as seen in Figure 3 (we will denote the phase to the stellar rotation period as  $\theta$ , with  $\theta=0$  corresponding to BJD=2455410.654). The transit depths phased to the stellar rotation period reach a maximum of approximately  $\sim 0.38 \pm 0.01\%$  from  $\theta = 0.54 - 0.74$ , compared to a minimum of approximately  $\sim 0.30 \pm 0.01\%$  at  $\theta = 0.04 - 0.24$ . Therefore, the transit depths are 25% deeper at one phase of the stellar rotation than another; this compares with the 30% signal reported by Kawahara et al. (2013) - most likely due to the fact that Kawahara et al. (2013) removes the rotational modulation by dividing through by the flux, rather than subtracting<sup>6</sup>. Although Kawahara et al. (2013) suggested

<sup>6</sup> In the original Kawahara et al. (2013) analysis the rotational modulation of the star was divided out to produce the flattened light curve using the routine *kepflatten*. Subtracting out, rather than dividing out, the rotational modulation of KIC 1255 is a significant improvement in our present work compared to the original Kawahara et al. (2013) study. Dividing through by the flux of the star that is displaying rotational modulation, imparts the ro-

that the deepest transit depths were roughly coincident with the minimum flux of the observed rotational modulation (and thus when the starspots were most visible), we illustrate in the top panel of Figure 3 and in Figure 4 that the starspots on KIC 1255 are highly variable. There is not a well defined, constant flux minimum of the rotational modulation. The effects of spots appear to be apparent at all phases of the stellar rotation period; if we are viewing the star in the equatorial plane then this corresponds to spots being visible at all longitudes of the star.

We also investigated changes in the shape of the transit profile of KIC 1255b, phased with the stellar rotation period. We split the data into discrete segments every 0.1 in stellar rotation phase,  $\theta$ . No obvious transit pro-

tational modulation signal into the transit depths of that star (as discussed in Section 3.1). Anywhere from  $<1\%$  to  $5\%$  of the modulation of the transit depths suggested by Kawahara et al. (2013) is likely due to this effect, compared to their reported 30% TDRM signal.

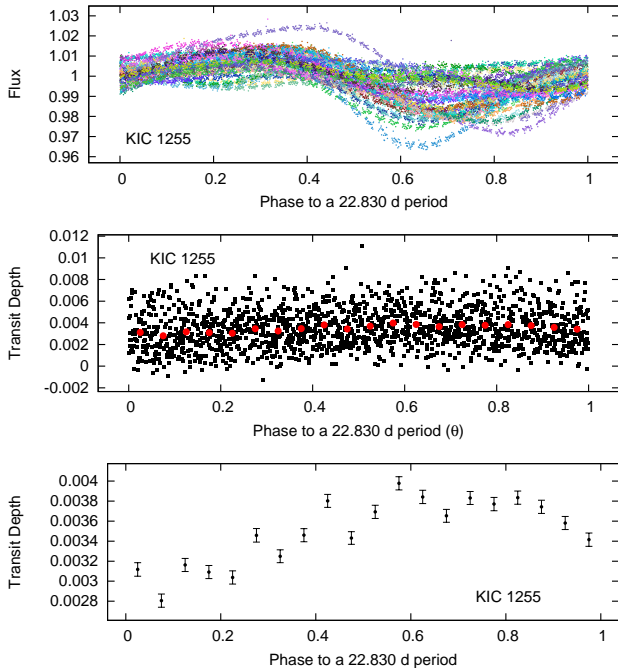


FIG. 3.— Top panel: The KIC 1255 *Kepler* long cadence photometry with the transits removed phased to the rotation period of the star. Each rotation period of the star is drawn with a different colour. Middle panel: The transit depths phased to the rotation period of the star (black points), and the transit depths binned every  $\phi=0.05$  in phase (red points). Bottom panel: The same binned transit depths phased to the stellar rotation period. Although the deepest transits appear to be roughly coincident with the mean minimum of the rotational modulation, in fact Figure 4 indicates that there is no well defined rotational modulation flux minimum for this star.

file shape changes were observed. We display the long cadence *Kepler* data for approximately the deepest ( $\theta = 0.6 - 0.7$ ) and shallowest ( $\theta = 0.1 - 0.2$ ) depths of the TDRM signal in Figure 5. The transit is deeper for  $\theta = 0.6 - 0.7$  compared to  $\theta = 0.1 - 0.2$ , but changes in the transit profile are not evident.

We have also investigated the strength of the KIC 1255 TDRM signal using different subsets of the *Kepler* data. The TDRM signal is stronger in the first-half of the data following the quiescent period, than in the second half. That is, we perform our analysis on the data from BJD - 2440000 = 15078 - 15600, and from BJD - 2440000 = 15600 - 16205 and display the results in Figure 6. The TDRM signal is significantly stronger in the left panels (*Kepler* data from BJD - 2440000 = 15078 - 15600), than in the right panels (*Kepler* data from BJD - 2440000 = 15600 - 16205). We discuss the possible importance of this in Section 3.2.

## 2.2. Lessons learned from other transiting planets orbiting spotted stars

We also apply our analysis to the photometry of several other spotted stars hosting transiting planets that have been observed with *Kepler*. Stars were chosen that display significant rotational modulation, that host a short-period transiting planet, and that have stellar rotation period that is much longer than the orbital period of the planet. These stars include: Kepler-17 (Desert et al. 2011), Kepler-78 (Sanchis-Ojeda et al. 2013), and HAT-P-11 (Bakos et al. 2010). The

TABLE 2  
FRACTION OF BOOTSTRAP ITERATIONS

Star	Fraction of bootstrap signals above the original signal
KIC 1255	0/1000
Kepler-17	0/1000
HAT-P-11	49/1000
Kepler-78	497/1000

stars Kepler-17 (Desert et al. 2011) and HAT-P-11 (Deming et al. 2011; Sanchis-Ojeda & Winn 2011) have been observed to display obvious occulted spots during transit. As Kepler-17 appears to be spin-orbit aligned, and there is a close commensurability of the orbital and rotation periods ( $\sim 8$  orbital periods to each rotation period), the spots of Kepler-17 appear to repeat every few transits, corresponding to a rotation period of the star (Desert et al. 2011). As these occulted spots will result in a slight mis-estimation of the transit depth, one would expect that the transit depth signal would be modulated by the rotation period of the star due to these occulted spots. Similarly, HAT-P-11, although it is spin-orbit misaligned (Deming et al. 2011; Sanchis-Ojeda & Winn 2011), has spots that appear to be relatively long-lived, and thus occulted spots may reappear a rotation period later, causing a possible TDRM signal. Unocculted starspots can also bias measurements of the transit depths, but our technique of subtracting out the rotational modulation should largely remove this bias, as discussed in Section 3.1.

To determine the impact of spots on the TDRM signal of these other stellar systems we repeat our analysis (Section 2.1) for these systems; minor differences in the parameters of our analysis to compensate for the properties of these different systems are summarized in Table 1. We display our analysis results in Figure 7 for Kepler-17, Figure 8 for HAT-P-11, and Figure 9 for Kepler-78. Kepler-17 displays an obvious peak in the Lomb Scargle periodogram at the rotation period of the star. There is a modest peak at the rotation period in the HAT-P-11 Lomb Scargle periodogram, while for Kepler-78 no peak is apparent at the rotation period. We note that the lack of a peak at the rotation period for Kepler-78, indicates that our technique for removing the rotational spot modulation does not induce a prominent signal into our measurements of the transit depths (at least at a detectable level for shallow transits, such as those displayed by Kepler-78). We present further evidence that our transit depths are not affected by leakage from the rotational modulation below in Section 2.3.

Ergo, the KIC 1255 TDRM signal does not appear to be entirely unique to KIC 1255; Kepler-17 displays a prominent correlation between the transit depths and the rotation period of the star due to occulted spots. This analysis indicates the possibility that occulted spots could be the source of the peak in the Lomb Scargle periodogram of the KIC 1255b transit depths near the stellar rotation period.

## 2.3. Is the KIC 1255 TDRM signal statistically significant?

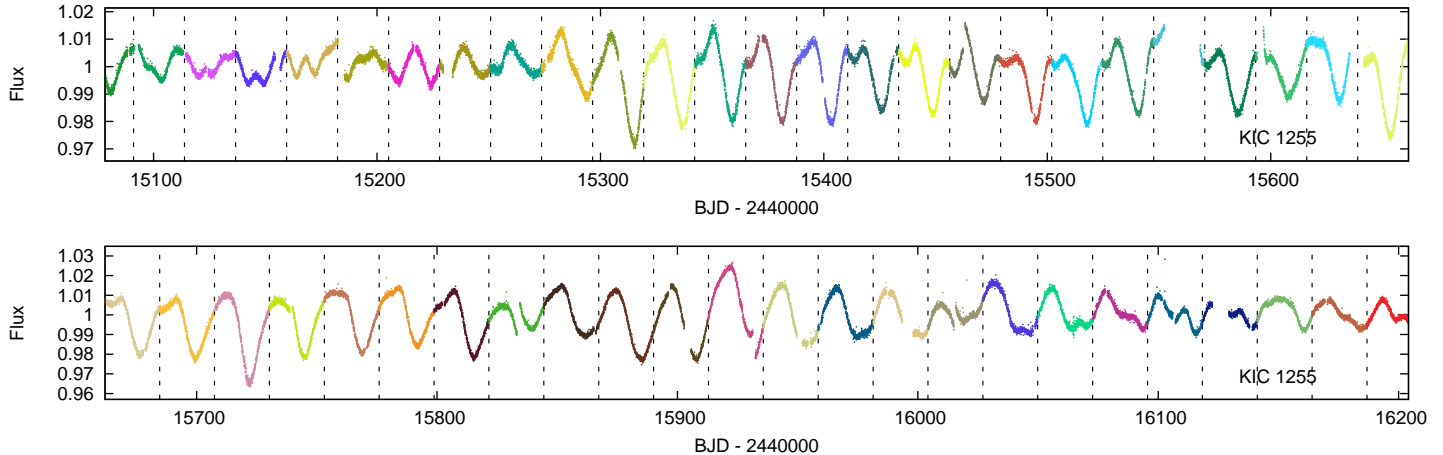


FIG. 4.— The long cadence *Kepler* photometry of KIC 1255 with the transits removed. The data are split into two plots, with the later dates at bottom. Each additional colour, and the vertical dashed lines, represent an additional rotation period of the star. The effects of spots on the light curve are visible at all phases of the apparent stellar rotation period, and therefore at all longitudes of the star if we are viewing the star edge-on.

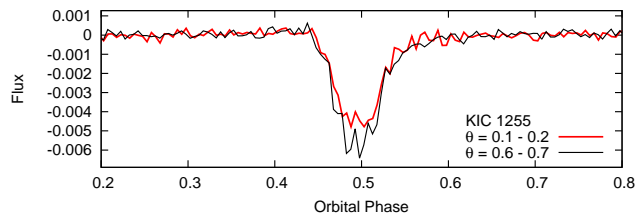


FIG. 5.— The long cadence *Kepler* photometry of KIC 1255 phased to the orbital period of the planet. In order to inspect transit profile differences with the stellar rotation period, we break the data into discrete segments with respect to the phase of the stellar rotation period,  $\theta$ . The mean transit profile for all the *Kepler* data from  $\theta = 0.1 - 0.2$ , corresponding to the shallowest transit depths of the TDRM signal, is displayed with the red solid line, while the mean transit profile for  $\theta = 0.6 - 0.7$ , corresponding to the deepest depths of the TDRM signal, is displayed with the black solid line. The mean transit profile is deeper, but not clearly different in shape for  $\theta = 0.6 - 0.7$ , compared to  $\theta = 0.1 - 0.2$ .

To determine if the TDRM signal is statistically significant, we repeat the analysis we present in Section 2.1, but randomly scramble and interchange the transits for one another. That is, after removing the rotational modulation using our cubic spline, we randomly scramble the data from a given transit for another using bootstrap techniques, reintroduce the rotational modulation, and then subject the data to our Section 2.1 analysis. To interchange the data during transits, once the rotational modulation has been removed using our cubic spline fit, we trade the data between the phases of  $\phi = 0.4 - 0.7$  of one transit with another transit that is chosen at random. The only obvious drawback of this technique is that the bootstrap data will no longer have the same strict  $\sim 29.4$  minute sampling at the beginning and end of the transit as the original KIC 1255 *Kepler* long cadence data. Nonetheless, we then compare the strength of the largest peak in the Lomb Scargle periodogram near the rotation period of the scrambled transits to that of the original unscrambled transits. We accept values for the peak of the Lomb Scargle periodogram within a day of the rotation period of the star, so we take the maximum Lomb Scargle periodogram power from periods of 21.9 - 23.9 d, compared to the  $\sim 22.9$  d rotation period of the star. Using these techniques we can determine what fraction of

the Lomb Scargle periodograms of the transit depths of KIC 1255b display a signal as large as what is observed simply by chance. We perform this bootstrap test on our KIC 1255b transits, excluding the data before and after the quiescent periods as in Figure 2; the results are similar if we include all the KIC 1255b transits, as in Figure 1.

A histogram of the maximum Lomb Scargle periodogram power near the KIC 1255 stellar rotation period for 1000 bootstrap iterations of our scrambled KIC 1255b transit depths is displayed in Figure 10. Zero of 1000 bootstrap iterations achieve a power as high as the original data. Therefore the KIC 1255 TDRM signal is highly significant. However, this highly significant signal could still be due to occulted spots.

To demonstrate this possibility, we repeat this analysis for Kepler-78, HAT-P-11, and Kepler-17. We accept values for the peak in the Lomb Scargle periodogram within a day of the rotation period for these stars. We summarize the results in Table 2, and display the results in Figure 10. Kepler-17 also displays a highly significant TDRM signal that, as previously discussed in Section 2.2, is likely simply due to occulted spots. The HAT-P-11 TDRM signal, again likely due to occulted spots, is detected at nearly the  $2\sigma$  level.

We note that as we reintroduce the rotational modulation after we have scrambled the transits in the bootstrap data-sets submitted to our analysis, the low power observed for many of the scrambled transit bootstrap datasets indicates that our analysis is efficient at effectively removing the impact of the rotational modulation on our measured transits depths. This further reiterates the point that the observed signal is not due to an artefact of leakage from the observed rotational modulation into our measured transit depths.

#### 2.4. Transit-timing analysis

We also perform a timing analysis of all the *Kepler* long cadence transits of KIC 1255b (Figure 1), and the *Kepler* transits excluding the quiescent periods (Figure 2). After removing the rotational modulation of KIC 1255 with our cubic spline as described in Section 2.1, we fit all the long cadence *Kepler* photometry of KIC 1255 with

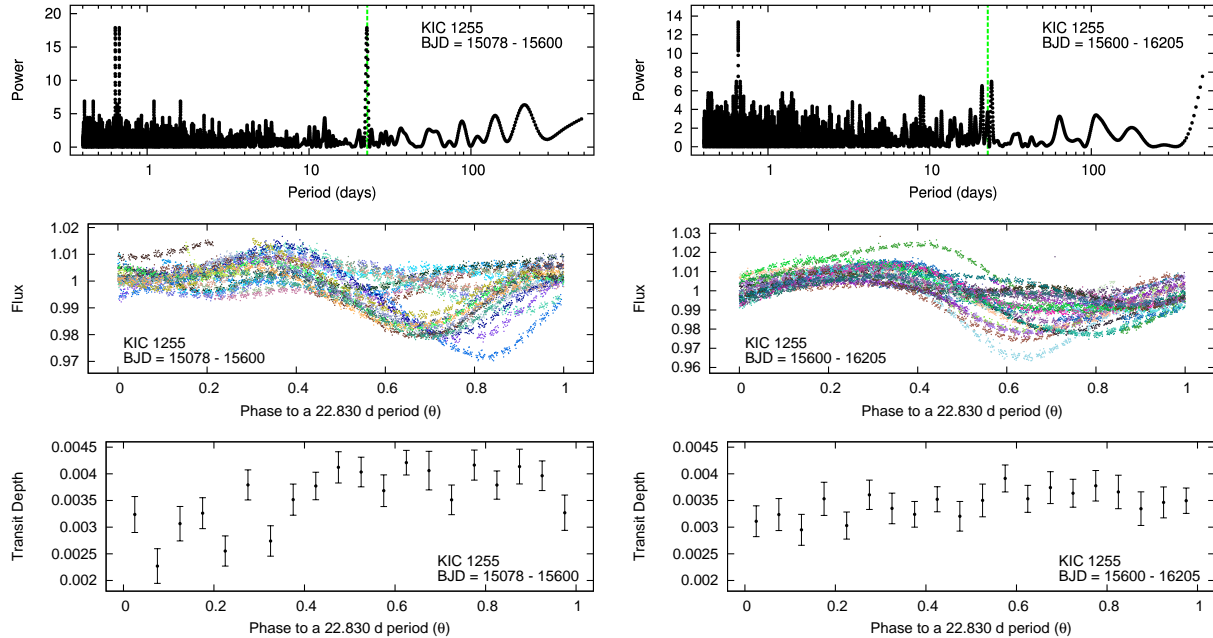


FIG. 6.— Our analysis for the first half of the *Kepler* long cadence data excluding the quiescent periods (BJD - 2440000 = 15078 - 15600; left panels), and for the second half of the *Kepler* long cadence data excluding the quiescent periods (BJD - 2440000 = 15600 - 16205; right panels). The top panels display the Lomb Scargle periodogram of the transit depths, with the stellar rotation period denoted by the vertical dotted green line. The middle panels show the *Kepler* long cadence data with the transits removed phased to the rotation period of the star, with each additional stellar rotation period plotted in a different colour. The bottom panels displays the transit depths phased to the stellar rotation period. The TDRM signal is significantly stronger in the early data (left panels), where a spot is visible at phase  $\theta \sim 0.2$ .

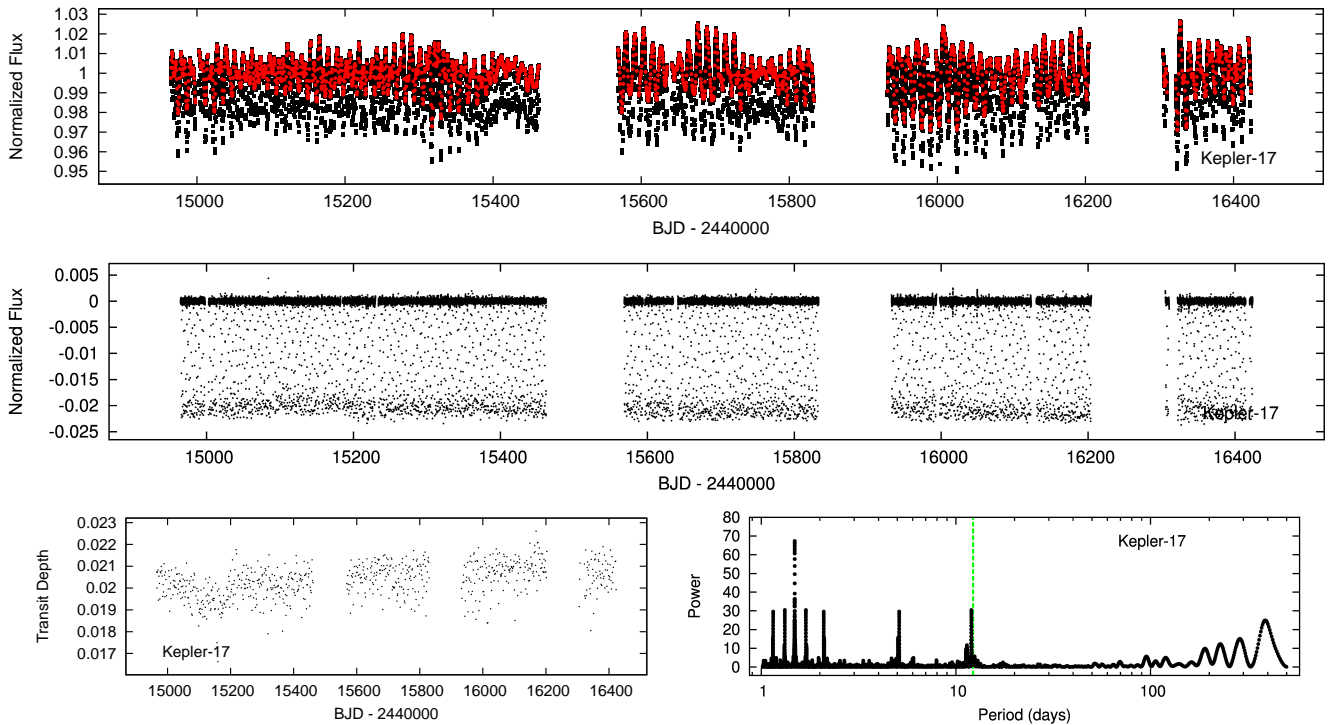


FIG. 7.— The Kepler-17 long cadence photometry (top), the photometry after the removal of the rotational modulation (middle), transit-depths (bottom left) and the Lomb Scargle periodogram of the transit depths (bottom right). The Figure format is identical to Figure 1. The vertical dotted green line in the bottom right panel indicates the  $\sim 12.3$  d rotation period of Kepler-17.

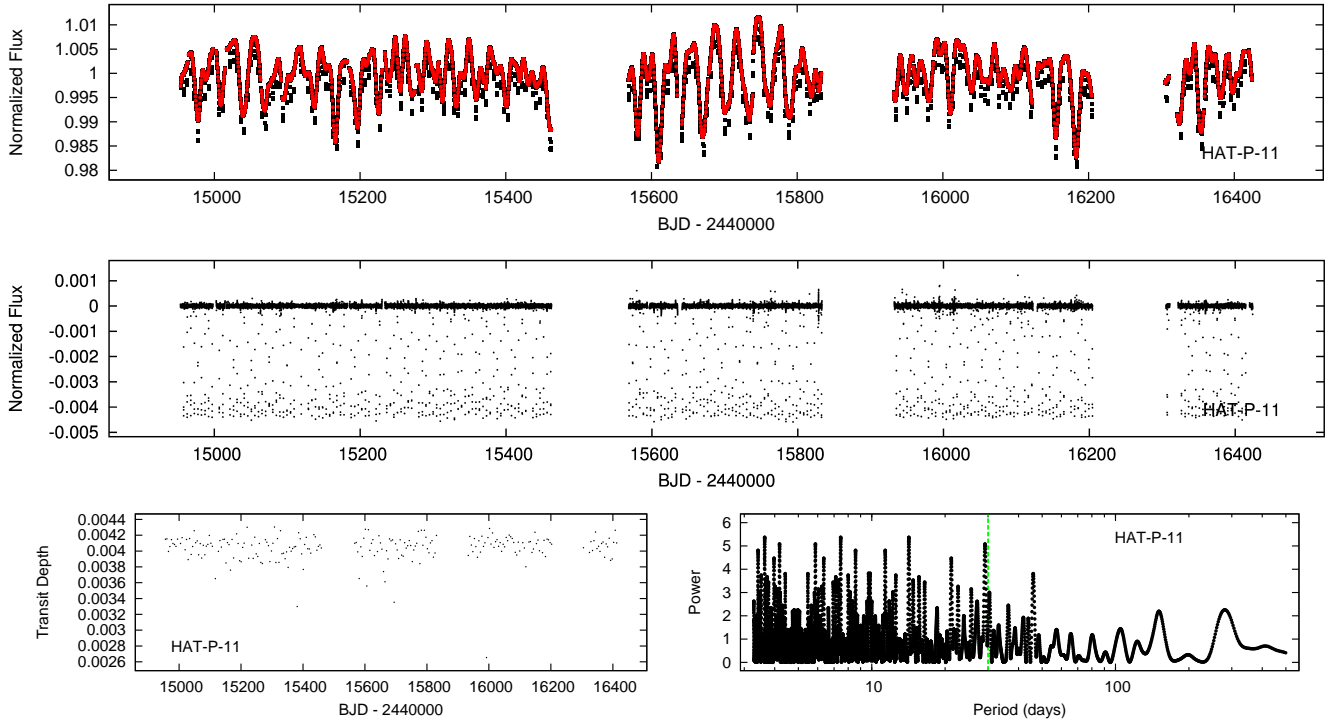


FIG. 8.— The HAT-P-11 long cadence photometry (top), the photometry after the removal of the rotational modulation (middle), transit-depths (bottom left) and the Lomb Scargle periodogram of the transit depths (bottom right). The Figure format is identical to Figure 1. The vertical dotted green line in the bottom right panel indicates the  $\sim 30.0$  d rotation period of HAT-P-11.

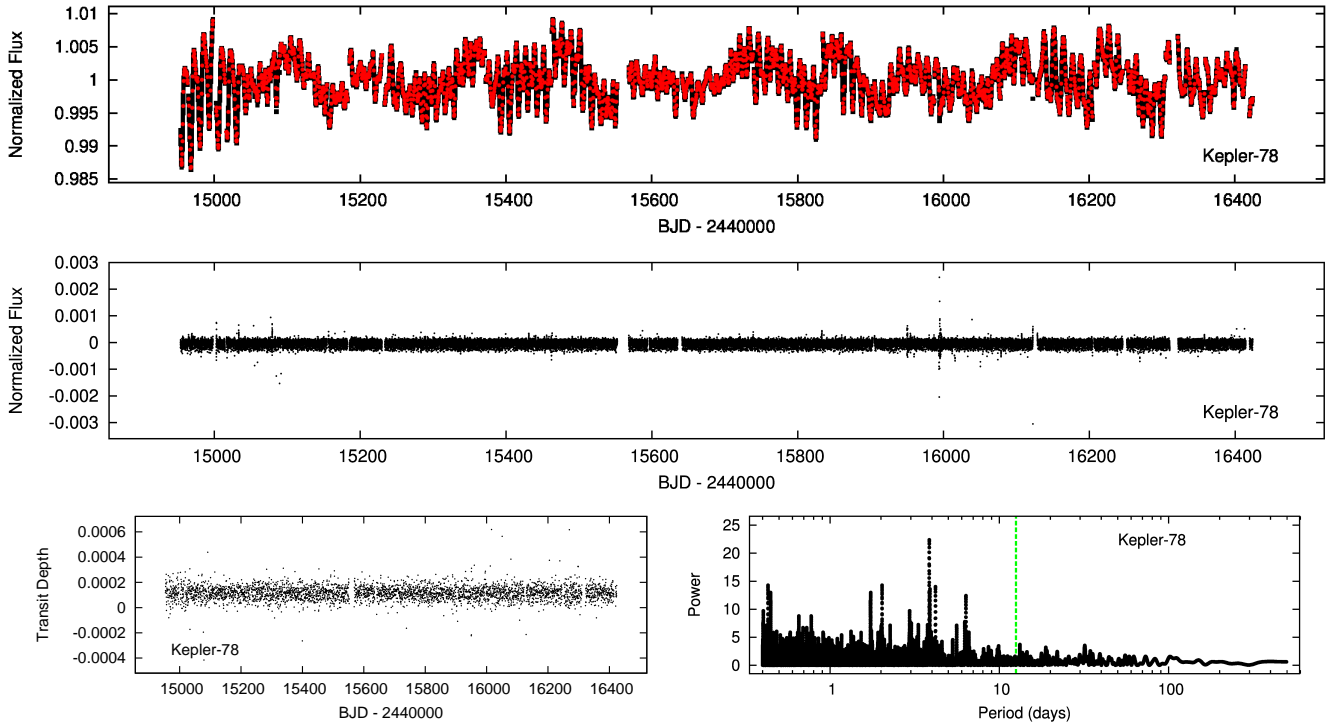


FIG. 9.— The Kepler-78 long cadence photometry (top), the photometry after the removal of the rotational modulation (middle), transit-depths (bottom left) and the Lomb Scargle periodogram of the transit depths (bottom right). The Figure format is identical to Figure 1. The vertical dotted green line in the bottom right panel indicates the  $\sim 12.8$  d rotation period of Kepler-78.

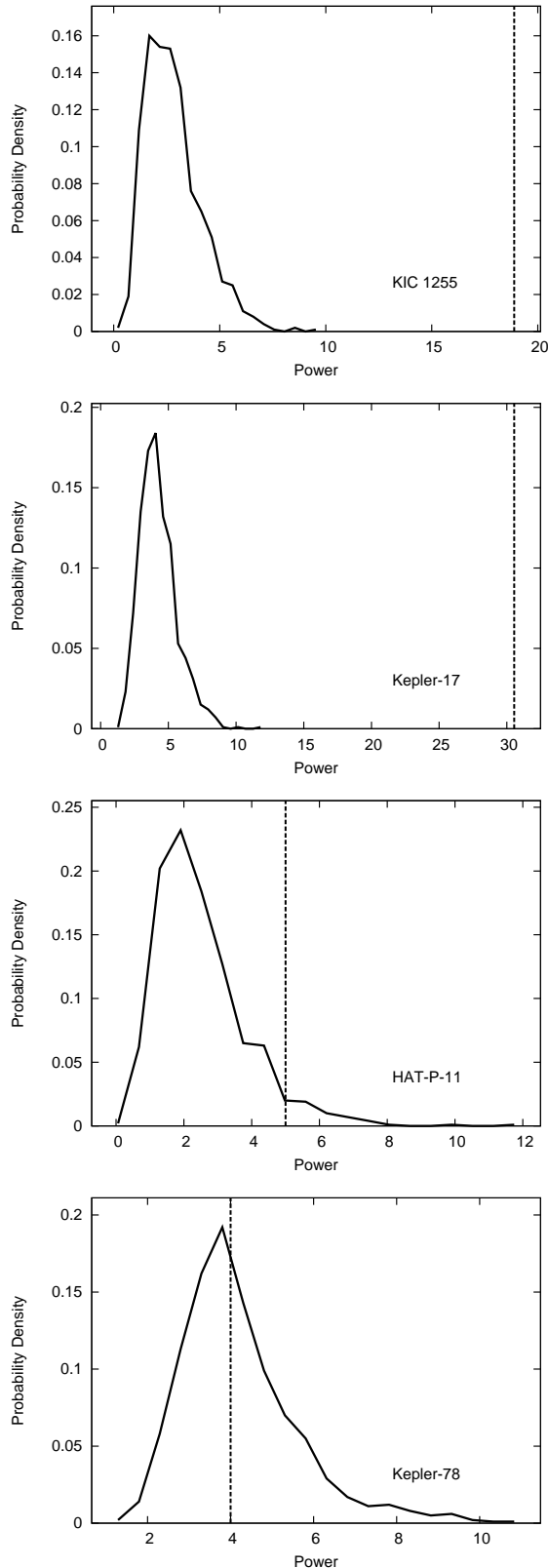


FIG. 10.— A histogram of the maximum Lomb Scargle periodogram power of the transit depths near the rotation period of the various stars following scrambling of the transits using bootstrap techniques. These stars, from top to bottom, are: KIC 1255, Kepler-17, HAT-P-11 and Kepler-78. The vertical dashed line displays the Lomb Scargle periodogram power for the original unscrambled data. The transit-depth rotational modulation signal is highly significant for KIC 1255, but it also highly significant for Kepler-17, where the signal is likely due to occulted spots.

a scaled and shifted version of the mean long cadence *Kepler* profile of the transit of KIC 1255b (as displayed in Figure 1 of Croll et al. 2014). We fit to Equation 1 of Croll et al. (2014) using Markov Chain Monte Carlo (MCMC) techniques as described in Croll (2006). We use MCMC chains with 150000 steps, which we found to be sufficient to return properly determined transit-times and errors. We place an a priori constraint on the offset from the expected mid-point of each transit of KIC 1255b of  $\pm 0.04$  d (58 minutes). We cut out all transits where the error on the timing of the transits exceeds 0.008 d ( $\sim 11.5$  minutes), leaving 1571 transit-times. This cut generally serves to cut out shallow transits, where it is difficult to identify the transit, and therefore challenging to return a useful limit on the timing of the transit mid-point.

The transit-timing results are displayed in the top and middle left panels of Figure 11 for all the transits, and for the transits excluding the quiescent periods. We also perform a Lomb Scargle periodogram on the transit-timing results to search for periodicities in the transit-timing signal. The results are shown in the top and middle right panels of Figure 11. The most prominent signal is at  $P \sim 563$  d. There is a modest signal at the rotation period of the star; we fit a sinusoid to this signal and place a  $3\sigma$  upper-limit on its amplitude of  $\sim 70$  s, after scaling the errors<sup>7</sup> so the reduced  $\chi^2$  is equal to 1.0 (the bottom panels of Figure 11). If we perform the same analysis on only the first half of the data (excluding the quiescent periods; BJD - 2440000 = 15078 - 15600), the associated  $3\sigma$  limit on the amplitude is  $\sim 160$  s.

#### 2.4.1. The orbital period and a limit on orbital decay

Our transit-timing analysis also allows us to measure the best-fit orbital period of KIC 1255b,  $P$ , and place a limit on the change of the period with time,  $\dot{P}$ , by fitting linear and quadratic functions to the integer transit number and the dates of the transit mid-points. The best-fit period is:  $P = 0.653,553,4(2)$  d, and the associated mid-point of the transit is BJD=2454968.9820(7)<sup>8</sup>, where the value in brackets in both cases is the  $1\sigma$  error on the last digit. Our best-fit value on the change in period with time divided by the period is:  $\dot{P}/P = 2.4 \pm 0.7 \times 10^{-9} d^{-1}$ , suggesting that, if anything, the period of the planet is increasing; therefore, there is no evidence that the orbit of the planet is rapidly decaying.

#### 2.4.2. Profile of Early, Normal and Late Transits of KIC 1255b

In order to determine if there is an astrophysical reason for the transit-timing variations, we also present the mean *Kepler* long cadence transit profile for those transits that occur earlier than expected, as expected, and later than expected. We present the “early” ( $O - C < -0.003$  d; 418 transits), “middle” ( $-0.003 < O - C < 0.003$  d; 832 transits) and “late” ( $O - C > 0.003$  d; 321 transits) transit profiles of KIC 1255b in Figure 12. The fact that the ingress of the “early” and “middle” transit profiles occur at approximately the same time is consistent

<sup>7</sup> We increased our error bars by a factor of  $\sim 2.5$ .

<sup>8</sup> The mid-point of the transit is defined as the minimum flux point of the mean *Kepler* Long cadence transit profile (Figure 1 of Croll et al. 2014).

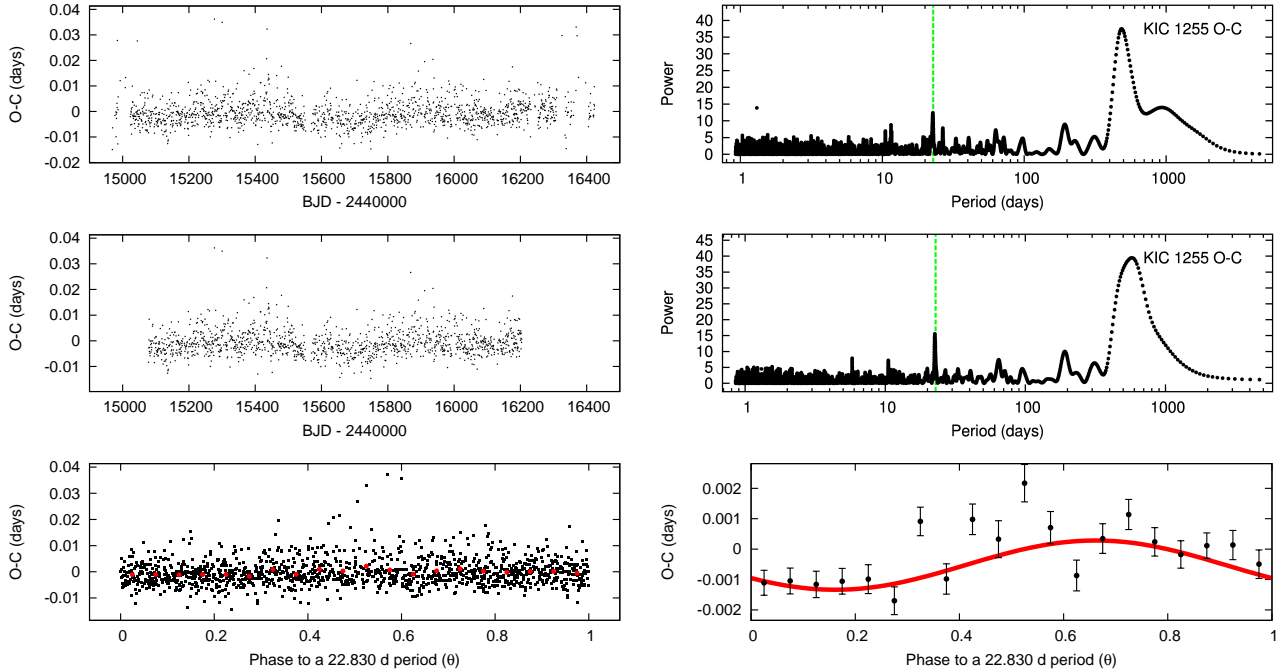


FIG. 11.— Top left panel: the transit timing analysis of all the transits of KIC 1255b. Top right panel: a Lomb Scargle periodogram of the O-C timing residuals of the transit-times of KIC 1255b. The vertical dotted green line denotes the rotation period of KIC 1255. Middle panels: the transit timing analysis for KIC 1255b excluding the quiescent periods (left panel), and the associated Lomb Scargle periodogram (right panel). Bottom left panel: the O-C transit times of KIC 1255b, excluding the quiescent periods, phased to the rotation period of the star (black points); the red points display the data binned every 0.05 in phase. Bottom right panel: The same binned data every 0.05 in phase, with the  $3\sigma$  upper limit on the best-fit sine-curve displayed with a red solid line.

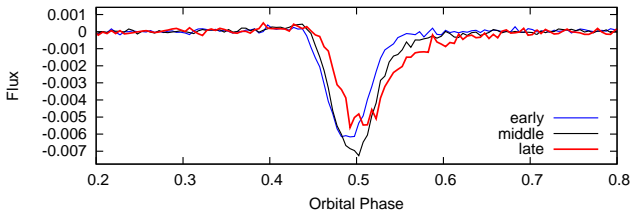


FIG. 12.— The long cadence *Kepler* photometry of KIC 1255 phased to the orbital period of the planet. The mean transit profile of the “early” transits ( $O - C < -0.003$  d) are shown with the blue line, the “middle” transits ( $-0.003 < O - C < 0.003$  d) are shown with the black line, and the “late transits ( $O - C > 0.003$  d) are shown with the red line.

with the candidate planet hypothesis with a tail of dust streaming behind it; in this scenario the ingress of the transit should occur no earlier than the ingress of the Mercury-sized planet across the stellar disk. The “late” transit profile could be due to an brief ( $\sim$ hour long) cessation of dust emission before the start of the ingress, leading to the dust tail trailing further behind KIC 1255b than usual<sup>9</sup>.

### 3. POSSIBLE EXPLANATIONS FOR THE KIC 1255 TRANSIT DEPTH ROTATIONAL MODULATION SIGNAL

#### 3.1. Could the TDRM signal be due to unocculted spots?

<sup>9</sup> On a more speculative note, the longer egress tail in the “late” transit profile could imply a higher than normal dust ejection rate for several hours prior to the transit followed by a period of exhaustion of the dust supply; similarly van Werkhoven et al. (2014) noted that there were a number of occasions in the *Kepler* data of “on-off” transit behaviour, where relatively deep transits of KIC 1255b were followed by undetectable transits.

The flux from a spotted star with a transiting planet,  $F(t)$ , at time  $t$  can be written as (Carter et al. 2011):

$$F(t) = F_o[1 - \epsilon(t)] - \Delta F(t) \quad (1)$$

where  $F_o$  is the flux of the unspotted and untransited star,  $\epsilon(t)$  is the fractional loss of light due to starspots, and  $\Delta F(t)$  is the flux blocked (or scattered in our case) by the planet during transit. As we normalize our signal by subtracting the mean of the long cadence photometry using our cubic spline fit at a given time,  $t$ , we essentially<sup>10</sup> subtract  $\epsilon(t)$ , and our measurement of the transit depths should be unaffected by unocculted spots<sup>11</sup>. The TDRM signal should not be due to unocculted spots.

#### 3.2. Could the TDRM signal be due to occulted spots?

Although the signal of a transiting planet occulting a cool starspot often leads to significant deviations (brightenings) in the transit light curve, these deviations are often short compared to the duration of the transit. However, due to the long cometary tail supposedly trailing behind the candidate planet KIC 1255b, if a spot occultation occurs, it should cause an anomalous brightening

<sup>10</sup> As Figure 4 indicates, KIC 1255 is a very spotted star, and it is possible that there are always spots visible on KIC 1255 during the *Kepler* light curve. If this is the case, we will have underestimated  $\epsilon(t)$ ; in that case our estimate of the transit depths of KIC 1255b will be systematically overestimated, but these depths will not be modulated at the rotation period, so this bias would not affect the rest of our conclusions.

<sup>11</sup> There will be a modest effect due to the normalization of the *Kepler* light curve by dividing through each *Kepler* quarter by its mean flux level. In this case, we would expect the transit depths to be modulated by at most a factor of  $\frac{1}{1-\epsilon(t)}$ , which for  $\epsilon(t) \sim 1-5\%$  is much less than the TDRM signal (Kawahara et al. 2013).

for a significant fraction of the transit duration. In this way, one might expect that occulted spots would play a larger role in modulating the transit depths of KIC 1255b at the stellar rotation period than would normally be expected for a transiting planet.

The fractional brightening of the normalized light curve during a transit due to occulted spots can be described as:

$$\delta F/F_* = \frac{A_{spot}(t)}{\pi R_*^2} \times \left(1 - \frac{I_s}{I_*}\right) \quad (2)$$

where  $A_{spot}(t)$  is the area of the spot projected onto the viewing plane that is occulted by the planet at time,  $t$ ,  $R_*$  is the radius of the star, and  $I_s$  and  $I_*$  are the intensity of the spot and star, respectively. The diffuse cloud believed to be trailing the candidate planet KIC 1255b will not block light from the star per se, but the scattering from the dust tail has a similar effect.

For the sake of simplicity, let us treat the cometary tail as a thin rectangular ribbon, and let us assume that the planet and its cometary tail are completely opaque, and the planet has a nominal transit depth of  $\Delta F(t)$ . Let  $\Delta F(t)$  be measured at the point when the cometary tail stretches completely across the star, and thus blocks out a width,  $w$ , on the star of  $2R_*$  and a height,  $h$ , where  $h \ll R_*$ . In that case the planet and tail cover a fractional area of the star, equivalent to the transit depth,  $\Delta F(t)$ , of:

$$\Delta F(t) = \frac{h \times w}{\pi R_*^2} = \frac{2h}{\pi R_*} \quad (3)$$

so,  $h = \pi \Delta F(t) R_*/2$ . In the Rappaport et al. (2012) cometary tail model of KIC 1255b, the scattering material is not believed to be completely opaque, but in that case this will just serve to enlarge  $h$ , and the effect will be qualitatively equivalent. Compared to the case where no spot is occulted, the expected increase in flux during transit due to the fraction of the spot that is occulted, of area  $A_{spot} = w_s \times h \sim 2R_s h$ , when  $h < R_s$ , is then<sup>12</sup>:

$$\begin{aligned} \delta F/F_* &\sim \frac{2R_s h}{\pi R_*^2} \times \left(1 - \frac{I_s}{I_*}\right) \\ &\sim \frac{2R_s \times \Delta F(t) \times \pi R_*/2}{\pi R_*^2} \times \left(1 - \frac{I_s}{I_*}\right) \\ &\sim \Delta F(t) \frac{R_s}{R_*} \times \left(1 - \frac{I_s}{I_*}\right) \end{aligned} \quad (4)$$

If we assume a single spot, then the size of the spot is proportional to the maximum fractional loss of light due to starspots for that rotational cycle,  $\epsilon$ :

$$\epsilon \sim \frac{R_s^2}{R_*^2} \times \left(1 - \frac{I_s}{I_*}\right) \quad (5)$$

and Equation (4) reduces to:

$$\delta F/F_* \sim \Delta F(t) \sqrt{\epsilon \left(1 - \frac{I_s}{I_*}\right)} \quad (6)$$

<sup>12</sup> If we instead assume a dust tail with an exponential falloff in density (with scale length  $\ell$ ), then Equation 4 would simply be multiplied by a factor of  $2\xi e^{-f\xi} (1 - e^{-2\xi})^{-1}$  where  $\xi \equiv R_*/\ell$ ,  $f \equiv L/R_*$ , and  $L$  is the distance between the planet and the starspot. This factor ranges between  $\sim 0.2$  and 2 for plausible choices of  $L$  and  $\ell$ , with a most likely value of  $\sim 1$ .

The rotational modulation that we observe is  $\sim 1-5\%$ ;  $\epsilon$  might actually be larger than this, as Figure 4 suggests a multitude of spots could be present on KIC 1255, and masking the true unspotted flux level of the star.

The most extreme assumption would be spots that are completely dark:  $I_s = 0$ . If we use this assumption and use an estimate of  $\epsilon \sim 4\%$ , this results in spots of size:  $R_s \sim 0.2 R_*$ . Using  $I_s = 0$  and  $\epsilon \sim 4\%$ , Equation (4) becomes simply:  $\delta F/F_* \sim 0.2 \Delta F(t)$ . That is the occulted spot signal, at its maximum, could represent a 20% brightening compared to the depth of the transit; the TDRM signal is 25% of the depth of the transit. Occulting a cool spot that modulates the flux of KIC 1255 at approximately the 4-6% level is therefore likely sufficient to explain the TDRM signal.

Occulted spots are known to cause modest transit-timing variations, generally on the order of a minute or less for conventional transiting planets (Barros et al. 2013); however, due to KIC 1255b's unique geometry and the putative cometary tail trailing behind it, we decided to explicitly model the effect of occulted spots on the transit light curve. We considered an occulted spot of radius in the range of  $R_s = 0.20 - 0.25 R_*$  with an internal surface brightness of 20% that of the host star ( $I_s/I_* = 0.2$ ). We then simulate a comet-like tail that is more narrow in height than  $R_*$  and allow it to pass over a limb-darkened<sup>13</sup> stellar disk at the same latitude as the spot. We adopt an exponentially decreasing dust density in the tail with increasing distance from the planet. The transit profile is then calculated for the chosen spot longitude; after which the profile is convolved with the *Kepler* long cadence integration time. Finally, the spot is stepped systematically in longitude and the resultant transit profiles are recalculated. We then subject these simulated profiles to a transit-timing analysis similar to what is used for the actual transits.

Our estimate suggests that occultations of a single spot causing 4% rotational modulation, results in approximately 25% variations in the transit depth, and transit-timing variations of up to  $\sim 240$  s. Transit-timing variations this large are ruled out by our  $3\sigma$  limit of 140 s on the peak-to-peak timing variations on the transit of KIC 1255b phased to the stellar rotation period (Figure 11) for the entire data-set. Such large transit-timing variations are not ruled out, however, if we only analyze the first-half of the *Kepler* long cadence data excluding the quiescent periods (BJD - 2440000 = 15078 - 15600), where the TDRM signal is stronger (Figure 6). Also, if multiple spots are occulted then transit depth variations of 25% can easily be caused without detectable transit timing variations.

### 3.2.1. Occulted Spots and the Phase of the TDRM Signal

The theory that the TDRM signal results from occulted spots is not immediately suggested by phasing the transit depths with the observed rotational modulation (Figure 3). If the TDRM signal results from occulted spots, one would naively expect that the shallowest transits would be found when the spots are most apparent; that is, since the minimum of the flux from the observed rotational modulation should coincide with the time the

<sup>13</sup> Using a linear limb-darkened profile with a limb-darkening coefficient of  $u=0.8$ .

spots are most visible, this should be when there is the highest likelihood of occulted spots. Figure 3 indicates that the shallowest transit depths are not observed near the average minimum of the observed stellar flux. However, as the transit of KIC 1255b likely only occults a small fraction of the surface of the star, it is very possible that the planet does not occult the largest spots visible on the star. As can be seen in Figure 4, spots appear to be visible at all stellar rotation phases, and therefore occulted spots that lead to shallower transit depths could occur at any stellar rotation phase. Ergo, a lack of correlation between the phase of the largest visible spots and the shallowest transit depths of KIC 1255b is not a good reason to reject the possibility that occulted spots might be causing the TDRM signal.

Figure 6 indicates that the TDRM signal is significantly stronger in the subset of the data from  $\text{BJD} - 2440000 = 15078 - 15600$ . The shallowest transit depths are observed at a phase compared to the stellar rotation period,  $\theta$ , of approximately  $\theta \sim 0.2$ . This coincides with a prominent spot that is apparent at that stellar phase that causes modulation of the light curve at approximately the 1% level. A spot causing a modulation of  $\epsilon \sim 1\%$  would result in transit depth variations of approximately  $\delta F/F_* \sim 0.1\Delta F(t)$  (assuming  $I_s=0$ ) - likely too small to explain the observed signal. However, as Figure 4 seems to suggest that KIC 1255 could be a very spotted star, it is possible that there are always a number of spots visible on KIC 1255 during the *Kepler* light curve. In that case, what we observe as an  $\sim 1\%$  decrement in flux due to rotational modulation, could actually be much larger; if a spot that actually represents approximately a 4% decrement in flux was occulted, this would be sufficiently large to explain the TDRM signal.

### 3.2.2. A Starspot model of a subset of the KIC 1255 photometry

To illustrate that what appears to be a 1% flux drop could actually be caused by a much larger spot, we fit a section of the KIC 1255 *Kepler* long cadence light curve with a Budding (1977) model using the techniques of *StarSpotz* (Croll et al. 2006; Croll 2006; Walker et al. 2007). We fit a subset of the long cadence *Kepler* photometry from  $\text{BJD}=2455397.2$  to  $\text{BJD}=2455462.3$ . We use values for the flux ratio of the spotted to unspotted photosphere,  $I_s/I_*=0.2$ , and the linear limb-darkening coefficient,  $u=0.8$ , similar to what were employed previously for another K-dwarf:  $\epsilon$  Eridani (Croll et al. 2006). We set the normalized flux of the unspotted photosphere as  $U = 1.04$ , an inclination angle to the line-of-sight of  $i=80^\circ$ , and place four starspots on the star. We display our possible spot model in Figure 13. The spot near the top of the star (the top visible portion of the star) causes a drop in flux of approximately 4% of the flux of the star. If this spot were occulted by the cometary tail trailing KIC 1255b, the effect would be large enough to explain the KIC 1255 TDRM signal. This is not in any way intended as a unique model to explain the observed rotational modulation of KIC 1255, but simply illustrative that our occulted spot explanation is plausible despite the shallowest transit depths being observed at a stellar rotational phase of  $\theta=0.2$ . There are likely a variety of other spot combinations that could serve to satisfy these conditions and could explain the KIC 1255

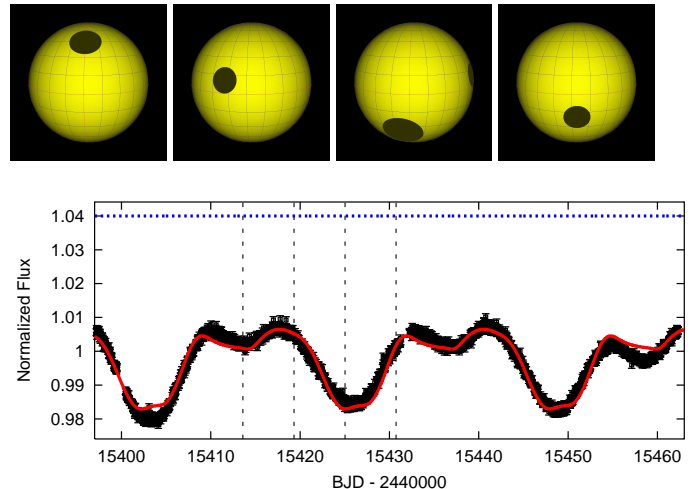


FIG. 13.— Top panels: Possible spot model of the rotational modulation of KIC 1255 as seen from the line of sight at stellar rotation phases  $\theta=0.15, 0.40, 0.65$  and  $0.90$  (from left). The bottom panel displays our *StarSpotz* fit (the red solid curve) to the *Kepler* long cadence photometry (black points with error bars) for a subset of the data. The blue horizontal dotted line displays the unspotted photosphere of the star. The vertical dotted black lines indicate phases  $0.15, 0.40, 0.65$  and  $0.90$  (from left). If the cometary tail of KIC 1255b transited the spots near the top of the visible portion of the star, this would cause sufficiently shallow transits to explain the KIC 1255 TDRM effect, despite the fact these spots only appear to cause 1% drops below the maximum flux level observed.

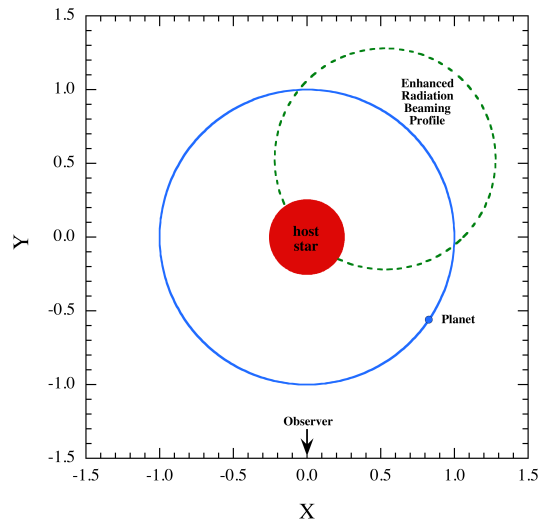


FIG. 14.— Schematic in the orbital plane of the KIC 1255 system with a hypothetical region of enhanced radiation through which the planet passes periodically. The green dotted curve represents the beaming function and is assumed to have a simple Lambertian profile. This is shown graphically as the distance from the origin (the middle of the host star) to the green curve as a function of angle from the stellar longitude where the enhancement peaks. The model discussed in the text assumes that the excess mass loss rate is proportional to the intensity of radiation in this region. Note that in this simple model there will be some enhancement in the mass loss rate over essentially half the orbit. The X and Y coordinates are normalized to the orbital radius of the planet.

TDRM signal.

### 3.3. Model with Periodically Enhanced Mass Loss

Inspired by the Kawahara et al. (2013) explanation for the TDRM signal – of an active longitude of enhanced ultraviolet or X-ray radiation or some other sort of star-

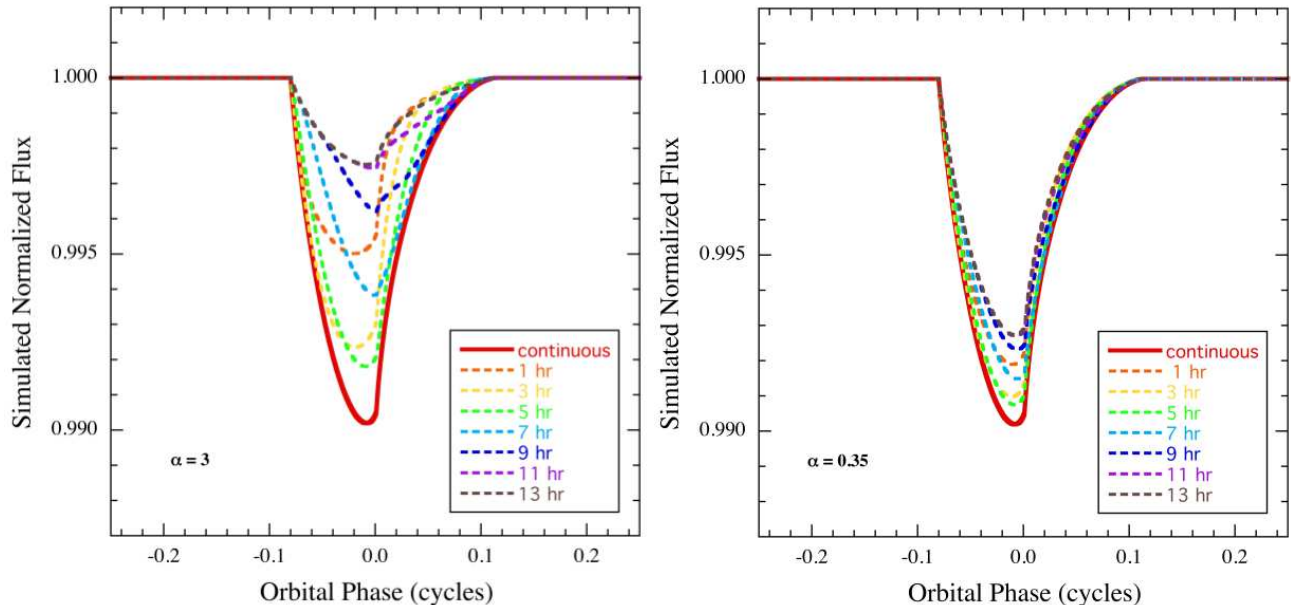


FIG. 15.— Dust-tail transit profiles for KIC 1255b calculated on the basis of the toy model discussed in the text. In this model, excess mass loss rates are stimulated each orbit when the planet passes through a beam of enhanced radiation which corotates with the host star. The color coding indicates the amount of time between passage through the center of the enhanced radiation field and the time to the following transit. After the dust-density profiles are computed (see text for details), we convolve the transmission profile with a limb-darkened stellar disk assuming an equatorial transit. The relative opacity of the dust is scaled until the resultant transit depth is about 1%. Left panel: the case where the mass loss rate at the peak of the enhanced radiation is a factor of  $1+\alpha=4$  times the steady state from the rest of the star. Right panel: the case where the enhanced mass loss rate is a factor of  $1+\alpha=1.35$  times the rest of the star.

planet interaction – in this section we attempt to evaluate the plausibility of a model wherein KIC 1255b passes through a region that drives enhanced mass loss from the planet. That is, we assume that once per synodic orbital period, the planet passes through an enhanced radiation field, leading to an increase in the mass loss rate in dust from the planet. A schematic of the scenario is shown in Figure 14. We make no attempt to describe the origin of this amplified radiation field or the details of how this leads to enhanced mass loss.

There are necessarily many things that we do not know about this hypothetical process of enhanced radiation from a specific longitude on the star leading to an increase in the mass loss rate from the planet, but we will choose an illustrative set of parameters that can hopefully show how such an effect might work. For one, the details of how radiation at various wavelengths interacts with the planet, heats the surface, and drives off heavy metal vapors are highly uncertain; they are discussed at length by Perez-Becker & Chiang (2013; see also Rappaport et al. 2012). The dynamics of the dust, once it condenses from the heavy metal vapor during the escape from the planet, are discussed in some detail by Rappaport et al. (2014) in the context of a second candidate “evaporating” planet (KOI-2700b).

In this simplistic toy model, which describes the effects of periodically enhanced mass loss, we assume that (1)  $\dot{M}_{\text{dust}}$  is directly enhanced by the instantaneous excess radiation field at the planet; (2) the radiation enhancement is described by a simple Lambertian beaming profile in orbital phase and centered at a particular stellar longitude leading to an enhanced mass loss rate that at its peak is a value  $\alpha$  above the steady state value (the steady state value is set to be unity); (3) there is a period of constant coasting velocity for the dust away from the

planet at several times the escape speed until the dust has reached several planetary radii; (4) the dust is subsequently subjected to only radiation pressure and to the gravity of the host star (with a ratio  $\beta$  for these two effects); and (5) the effective scattering cross section of the dust decays exponentially in time with a time-constant,  $\tau_{\text{dust}}$ , due to sublimation. The longitude where the enhanced radiation is centered (see Figure 14) is assumed to corotate with the host star every  $P_{\text{rot}} = 22.9$  days.

For each assumed longitude where the enhanced radiation is centered, we compute how far the dust has moved down the tail by the time of the next planetary transit. The motion of the dust particles in the tail, relative to the planet, was determined by integrating Equation (3) of Rappaport et al. (2014). The density of a parcel of dust is taken to be proportional to the radiation field at the planet at the time the dust was emitted, and to have decayed exponentially in time. The two key parameters in this ad hoc model are the ratio of radiation pressure to gravity,  $\beta$ , which we arbitrarily take to be 0.07 (see Appendix B of Rappaport et al. 2014), and the exponential decay time for the effective cross section of a dust grain,  $\tau_{\text{dust}}$ , which we arbitrarily take to be 2.5 hours. The dust extinction at that location in the tail is taken to be proportional to the dust density, and the attenuation profile is thereby calculated. Finally, we move the longitude of the centroid of the enhanced radiation beam (as a proxy for the rotating host star), and repeat the calculation.

The results are presented in Figure 15. We show a series of calculated transit profiles for different time intervals between the planet’s passage through the enhanced radiation zone and the time of the next transit. To produce these curves, we have taken each of the simulated dust-density profiles and convolved it with a limb-

darkened star<sup>14</sup>. The two cases shown are for a peak mass loss rate that is a factor of  $1+\alpha=4$  times the steady state, unenhanced mass loss rate from the rest of the star (left panel), and another that is  $1+\alpha=1.35$  times the steady state (right panel). The heavy red curve in each plot is the expected transmission profile, using the same model, except that the enhanced radiation zone is made so large as to produce a nearly continuous outflow of dust. The left panel of Figure 15, especially, indicates that not only does the proposed mechanism cause transit-depth variations, it can also lead to transit-timing and transit-profile variations. We note that our  $\alpha=0.35$  model produces transit depth variations on the order of 27%, similar to the KIC 1255 TDRM signal.

We conclude from these calculations that such a hypothetical model of enhanced driven mass loss, at a preferential stellar longitude that rotates with the host star, can quite naturally produce systematic changes in the transit depth, of the correct magnitude and in phase with the 22.9-day rotation period. For our 1.35-times enhanced mass loss model, the shapes of the transit profiles do not change dramatically with the 22.9-day orbital phase. This is consistent with the fact that no obvious transit profile changes were visible in the KIC 1255 *Kepler* long cadence photometry (Figure 5). We note that in spite of the lack of predicted dramatic changes in transit profile, there might be imperceptible changes that can still lead to measurable transit-timing variations — and we can check this with our model. After convolving our profiles with the *Kepler* long cadence integration time, we subjected our profiles to a transit timing analysis. Our model with a mass-loss enhancement of 1.35-times the steady-state ( $\alpha=0.35$ ; right panel in Figure 15), produces transit depth variations on the order of  $\sim 27\%$ , and transit-timing variations on the order of  $\sim 205$  s. This value is marginally above our stringent  $3\sigma$  limit of 140 s on the peak-to-peak timing variations on the transit of KIC 1255b phased to the stellar rotation period for all the data (Figure 11). If we only analyze the first half of the *Kepler* long cadence data (excluding the quiescent periods; BJD - 2440000 = 15078 - 15600), where the TDRM signal is stronger (Figure 6), such transit-timing variations are not ruled out. Although the Kawahara et al. (2013) proposed mechanism would naturally lead to transit-timing variations, our analysis indicates that these transit-timing variations could be small enough that they could have escaped detection in the *Kepler* long cadence data.

We acknowledge that there are a number of parameters associated with our toy model that one could quibble with; nonetheless, the above simulation and ‘analysis’ suggests that it is possible that an active longitude could drive enhanced mass loss and transits that are 25% deeper at one stellar rotation phase than another, with transit-timing variations that are small enough that they would not have been ruled out by the *Kepler* long cadence photometry of KIC 1255. We therefore cannot rule out the validity of the model proposed by (Kawahara et al. 2013).

### 3.3.1. Validity of the ultraviolet flux as a driver of an enhanced mass loss rate

<sup>14</sup> Again using a linear limb-darkened coefficient of  $u=0.8$ .

The mechanism most discussed for removing gaseous heavy metal material from KIC 1255b has been a Parker-type wind. This wind is generated by heating of the base of the atmosphere by the broadband radiation from the parent star which drives a hydrodynamic outflow (Rappaport et al. 2012; Perez-Becker & Chiang 2013). It is also possible that the mass loss rate could be supplemented, or even dominated, by photoevaporation of the planetary atmosphere by the X-ray and/or extreme ultraviolet (EUV) flux from the host star as alluded to in the model proposed by Kawahara et al. (2013). We can utilize the prescription of Sanz-Forcada et al. (2011) for estimating the nominal EUV luminosity of KIC 1255:

$$\log(L_{\text{EUV}}) \simeq 29.1 - 1.2 \log(\tau)$$

where  $\tau$  is the age of the star in Gyr, and we adopt a gyrochronological age of 1 Gyr (Barnes 2007). If we further assume that the EUV flux dominates over the X-ray flux (Sanz-Forcada et al. 2011), we can utilize the expression for photoevaporative mass loss rates following Watson et al. (1981), Lammer et al. (2003), and Sanz-Forcada et al. (2011), to write

$$\dot{M}_{\text{evap}} \simeq 6 \times 10^{11} \left( \frac{F_{\text{EUV}}}{2 \times 10^5 \text{ ergs sec}^{-1} \text{ cm}^{-2}} \right) \left( \frac{5g \text{ cm}^{-3}}{\rho_p} \right) \text{ g s}^{-1}$$

where  $\rho_p$  is the mean density of the planet. This is sufficient from an energetics point of view to eject the inferred mass loss rates from KIC 1255b (Rappaport et al. 2012). We might therefore conclude that a persistent longitude on the host star with excess EUV emission might plausibly account for the TDRM signal. However, this mechanism is likely to be much more efficient at removing lighter, higher-velocity molecules — such as H, He, and H<sub>2</sub>O — than the heavy metal molecules that would be needed to form dust from the atmosphere of a rocky planet. Thus, it may be that photoevaporation of rocky planets may not be nearly so efficient as it could be for gas giants, therefore calling into question the validity of this model in regard to the supposedly sub-Mercury-mass KIC 1255b (Croll et al. 2014).

### 3.3.2. GALEX observations of KIC 1255

Another way to constrain the Kawahara et al. (2013) model that there is an active longitude on KIC 1255 that is displaying enhanced ultraviolet or X-ray emission is to actually observe KIC 1255 at these wavelengths to see if the flux is modulated at the rotation period of the star. The *Galaxy Evolution Explorer* (GALEX; Martin et al. 2003) performed ultraviolet observations of the *Kepler*-field, but these observations were not able to detect KIC 1255; there is no near-ultraviolet source at the position of KIC 1255 to a magnitude limit of  $m_{AB} < 22$  mag. As KIC 1255 is relatively faint, this does not rule out a moderately young, active star (Jamie Lloyd & Everett Schlawin, private communication).

## 4. SUMMARY

In this work we attempted to confirm the claimed signal of Kawahara et al. (2013) wherein the depth of the transits of KIC 1255b were correlated with the phase of the stellar rotation. We confirmed that there is indeed a robust, statistically significant correlation between the depths of KIC 1255b’s transits and the stellar rotation

period. This signal is not due to the leakage of the rotating spot signal into our measurement of the transit depths, or due to unocculted starspots. The transits of KIC 1255b are approximately 25% deeper at one stellar rotation phase than another. We show that the effect is stronger in the first-half of the *Kepler* light curve than in the second-half. We also perform a transit timing analysis of the transits of KIC 1255b and are able to place a  $3\sigma$  upper-limit on the peak to peak amplitude of these variations phased to the stellar rotation period of  $\sim 140$  s.

To help us understand the transit depth rotational modulation signal, as KIC 1255 is a very spotted star with rapidly evolving spots, we also searched for such signals in the *Kepler* light curves of several other spotted stars with transiting planets. A transit depth rotational modulation signal is observed in two other spotted stars with transiting planets that feature starspot occultations by the transiting planet. Due to the unique geometry of the candidate disintegrating planet KIC 1255b, if its dust tail occults a cool starspot, we show that the anomalous brightening during transit due to the occultation will persist for a longer fraction of the transit than for other transiting planets. A likely explanation for this signal is that the dust tail trailing KIC 1255b occults starspots, leading to shallower transits at certain stellar rotation phases. Such a model could lead to large transit-timing variations (up to  $\sim 240$  s); however, if the planet is occulting a number of small spots, the associated transit-timing variations could be much smaller, and therefore we feel this model is arguably consistent with our upper limit on timing variations of the transits of KIC 1255b.

We also investigate the suggestion that the transit depth rotational modulation signal could be due to an active longitude on the star that causes an increased mass loss rate from the planet; we employ a toy model that suggests that such a model could naturally lead to transit depth variations similar to what we observe. This model could similarly lead to transit-timing variations ( $\sim 205$  s variations), although such variations could have been small enough that they escaped detection in the *Kepler* long cadence photometry.

For these reasons we believe that both occulted spots and an active region driving increased mass loss remain viable options to explain the Transit Depth Rotational Modulation signal. However, as there is not currently any empirical evidence that there is an active region on KIC 1255 that is exhibiting enhanced ultraviolet or X-ray flux, we believe the occulted spot scenario provides the simplest explanation for the observations. Therefore, our preferred explanation for the statistically significant correlation between the KIC 1255b transit depths and the phase of the stellar rotation period is that the cometary tail trailing KIC 1255b occults cool starspots, leading to slightly shallower transit depths during these occultations.

B.C.'s work was performed under a contract with the California Institute of Technology funded by NASA through the Sagan Fellowship Program. We thank Roberto Sanchis-Ojeda & Kevin Schlaufman for helpful discussions that contributed to this work. We thank Jamie Lloyd & Everett Schlawin for sharing their analysis of the GALEX observations of KIC 1255.

#### REFERENCES

- Bakos, G.A. et al. 2010, ApJ, 710, 1724  
 Barnes, S.A. 2007, ApJ, 669, 167  
 Barros, S.C.C. et al. 2013, MNRAS, 430, 3032  
 Borucki, W.J. et al. 2009, Science, 325, 709  
 Brogi, M. et al. 2012, A&A, 545, L5  
 Budaj, J. 2013, A&A, 557, A72  
 Budding, E. 1977, Ap&SS, 48, 207  
 Carter, J.A. et al. 2011, ApJ, 730, 82  
 Croll, B. et al. 2006, ApJ, 648, 607  
 Croll, B. 2006, PASP, 118, 1351  
 Croll, B. et al. 2014, ApJ, 786, 100  
 Czela, S. et al. 2009, A&A, 505, 1277  
 Deming, D. et al. 2011, ApJ, 740, 33  
 Desert, J-M. et al. 2011, ApJS, 197, 14  
 Kawahara, H. et al. 2013, ApJ, 776, L6  
 Koch, D. G., Borucki, W. J et al. 2010, ApJ, 713, L79  
 Lammer, H. et al. 2003, ApJ, 598, L121  
 Lomb, N. R. 1976, Ap&SS, 39, 447  
 Martin, C. et al. 2003, in Society of Photo-Optical Instrumentation Engineers (SPIE) Conference Series, Vol. 4854, Society of Photo-Optical Instrumentation Engineers (SPIE) Conference Series  
 Perez-Becker, D. & Chiang, E. 2013, MNRAS, 433, 2294  
 Rappaport, S. et al. 2012, ApJ, 752, 1  
 Rappaport, S. et al. 2014, ApJ, 2014, 784, 40  
 Sanchis-Ojeda, R. & Winn, J.N. 2011, ApJ, 743, 61  
 Sanchis-Ojeda, R. et al. 2013, ApJ, 774, 54  
 Sanz-Forcada, J. et al. 2011, A&A, 532, A6  
 Scargle, J.D. 1982, ApJ, 263, 835  
 Smith, J.C. et al. 2012, PASP, 124, 1000  
 Stumpe, M.C. et al. 2012, PASP, 124, 985  
 van Werkhoven, T.I.M. et al. 2014, A&A, 561, A3  
 Walker, G.A.H. et al. 2007, ApJ, 659, 1611  
 Watson, A.J. et al. 1981, Icar, 48, 150